

MIMO PLC Channel Modeling on Indian Residential Networks

Shashidhar Kasthala.

*Department of Electrical and Electronics Engineering
Karpagam University
Karpagam Academy of Higher Education
Coimbatore, India.*

Orcid Id: 0000-0002-6801-5749

GKD Prasanna Venkatesan

*Research and Development Cell
SNS College of Engineering
Coimbatore, India.*

Orcid Id: 0000-0002-0638-1938

A Amudha

*Department of Electrical and Electronics Engineering
Karpagam University
Karpagam Academy of Higher Education
Coimbatore, India.*

Orcid Id: 0000-0001-5138-716x

Abstract

To fully evaluate the potential of MIMO technology in power line communication, the channel properties should be thoroughly analyzed. In this paper, efficacy of MIMO technology is studied the Indian residences. For this, the frequency response of the channel, the stationary noise and the Impulsive noise are extensively measured. The frequency response is modeled using the multi-conductor transmission line theory and both the noises are statistically modeled. The channel capacity and average channel gain of the MIMO power line communication is also estimated.

Keywords: Average Channel Gain, Noise Model, MIMO PLC Channel, Singular Value Decomposition.

INTRODUCTION

Though, the power line is hostile to data transmission, the wide coverage of the network as always attracted by the researchers. For this reason, the PLC is termed as last mile alternative for other contemporary communication technologies [1]. Implementation of MIMO technology in PLC has also the advantage of achieving higher speed and maximum data rate.

In a typical single-input single-output (SISO) PLC, the data is transmitted/ received between Live (L) and Neutral (N) ports. But for MIMO PLC, the earth (E) wire will also be used, in addition, for data communication. Since, the single phase wiring in Indian residences, generally, contains all the three wires; a 3x3 MIMO communication should be possible. But, as per Kirchhoff's current law, only N-1 i.e., 2 ports can be used for transmitting and/or receiving data.

To develop an effective and reliable PLC system, the power line channel should be meticulously analyzed in terms of noise, attenuation and impedance mismatches. For this, ETSI has launched STF 410 to analyze the channel properties in Europe [2][3][4]. In similar lines, this paper analyses the efficacy of PLC in Indian residences.

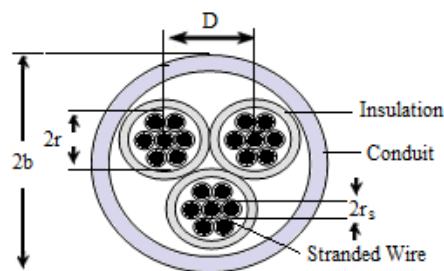


Figure 1: Typical residential wiring

The power line channel models, developed so far, are basically an extension of either top-down approach or bottom-up approach. The former is based on the concept of multipath propagation and is built on extensive measurements carried out and the latter is using the transmission line theory built on the data obtained from topology of the network [5].

Though the top-down procedure involves simple computations compared to bottom-up approach, it may not be the best choice, when a large diverse network is to be dealt with [6]. Hence for modeling, the MTL theory is preferred in this paper [7].

The EMI in the power lines can be modeled using the Middleton Class A model or the Markov-Middleton Model. The former is a simple model with only three parameters and the latter has memory component in addition. But as per [8],

stochastic models are more suitable and represent the complete behavior of noise.

In this paper, an experimental setup is developed in an Indian residence to characterize the MIMO PLC. With the setup, the Channel Frequency Response (CFR) and the impedance of the electrical network is measured. In addition to this, the stationary noise and impulsive noise on the power line is also measured and statistically modeled. The measurements for this are carried out using a R&S ZVL network analyzer, R&S FSL spectrum analyzer and Agilent DSOX3014A Oscilloscope.

In this paper the CFR is modeled based on the intrinsic parameters estimated from the physical conditions of the network. Though a difference in measured and simulated CFR is noticed, the Average Channel (ACG) for both is almost same. The variation in response can be attributed to the dynamic nature of the network and the assumptions made in this work. For evaluating the channel capacity of modeled channel, the noise is obtained from the statistical analysis.

The succeeding sections of the paper are organized as follows. In section II, the Indian residential networks are studied in detail for implementation of PLC. In section III, the channel modeling of MIMO PLC channels is carried out. In section IV, experimental analysis was carried out to measure the CFR, stationary noise and Impulsive noise. In section V, the CFR is modeled and the channel capacity and average channel gain were simulated.

RESIDENTIAL NETWORKS FOR PLC

The Indian residential network, typically, contains live, neutral and earth wires, of equal cross-section, as shown in Fig. 1. These wires are loosely twisted and are placed in a conduit pipe between the main distribution panel (entrance of the building) and the power outlets located across the building. These power outlets can be of 6 A or 16 A depending upon the appliance to be connected and hence the wiring cross-section connecting these outlets may not be uniform.

The loads connected to the power lines are also very diverse in nature and so is their affect on the power line channel. Though, in general, the appliances require all the three wires, the lighting loads or low power loads need only live and neutral. Due to this, the CFR is varied for different ports of the power line channel.

To model a MIMO PLC system, the four fundamental parameters resistance (R), inductance (L), capacitance (C) and conductance (G) need to be estimated for the three different wires of the cable [9].

A. Distributed Parameters

The four primary parameters of a power lines are measured for a two-wire transmission line and then extended to a 3-core

cable.

The Resistance of the single wire is given as

$$R = \frac{1}{\pi r \delta \sigma} \left[\frac{\frac{D}{2r}}{\sqrt{\left(\frac{D}{2r}\right)^2 - 1}} \right] \quad (1)$$

The skin depth is obtained by

$$\delta = \frac{1}{\sqrt{\pi f \mu \sigma}} \quad (2)$$

Here r and D being the conductor radius and distance between the conductors respectively, σ and μ being cable conductivity and permeability respectively.

However, since stranded wiring with radius r_s is used, the correction factor will be

$$X_{RS} = \frac{\left[\cos^{-1}\left(\frac{r_s - \delta}{r_s}\right) r_s^2 - (r_s - \delta) \sqrt{r_s^2 - (r_s - \delta)^2} \right]}{2 r_s \delta} \quad (3)$$

The total inductance of a cable is given as

$$L = \frac{\mu}{\pi} \cosh^{-1}\left(\frac{D}{2r}\right) + \frac{R}{2\pi f} \quad (4)$$

The correction factor for the stranded conductor is given as

$$X_{LS} = \frac{n_s \pi r_s^2}{\pi r^2} \quad (5)$$

Here n_s represent the strands in the conductor.

As per [10], the inductance is directly affected due to skin effect and the correction factor is given as

$$X_{LK} = \frac{\delta}{0.135 \times 0.53 \times r_s} \quad (6)$$

In addition to (5) and (6), the earth wire and the cable geometry will also affect the inductance.

The capacitance of the cable is affected by the twisting of the wires, cable geometry, and conduit capacitance. The correction factor for the dielectric constant (ϵ_{eq}) of a power line with T twists is given as [11]

$$X_{TW} = 0.45 + \left(\tan(T \cdot \pi \cdot D) \times \frac{180}{\pi} \right)^2 \times 10^{-3} \quad (7)$$

For the geometry of the cable, the three wires are not symmetrically placed. The capacitance between any two conductors is given as

$$C_{Cbl} = \frac{\pi \epsilon_0 \epsilon_{eq}}{\ln\left[\frac{D}{2r} + \sqrt{\left(\frac{D}{2r}\right)^2 - 1}\right]} \quad (8)$$

Here, ϵ_{eq} is the equivalent dielectric constant obtained by

$$\epsilon_{eq} = 1 + X_t(\epsilon_r - 1) \quad (9)$$

As per [12], the capacitance is given as

$$C = 3 \frac{C_{Cbl}}{2} + \frac{C_{cndt}}{2} \quad (10)$$

Where $C_{conduit}$ is the capacitance between the wires and the

conduit which is given as

$$C_{conduit} = \frac{\pi \epsilon_c}{\ln\left(\frac{b}{r}\right)} \quad (11)$$

Here, with a conduit radius of b , the permittivity includes the air in between the cable and conduit. The cable conductance is expressed as

$$G_{cable} = 2\pi f \cdot C_T \cdot \tan\delta \quad (12)$$

The cable conductance is influence by the conduit and can be directly derived from the capacitance

$$G = \frac{G_{cable} \cdot C_T}{C_{cable}} \quad (13)$$

B. MIMO PLC System

The data through power line can be transmitted through a differential signal between L-N or L-E or N-E. For SISO communication, signal is fed through any one the port and for MIMO communication, the signal is fed through multiple ports simultaneously.

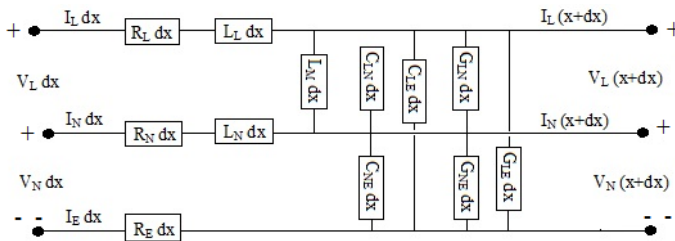


Figure 2: MIMO PLC system

From the Fig. 2 and the parameters obtained from (1) to (13), the p.u length parameter matrices for R, L, G and C in terms of Ω/m , H/m, F/m and S/m respectively are

$$R = \begin{bmatrix} R_L + R_E & R_E \\ R_E & R_N + R_E \end{bmatrix} \quad (14)$$

$$L = \begin{bmatrix} L_L & L_M \\ L_M & L_N \end{bmatrix} \quad (15)$$

$$C = \begin{bmatrix} C_{LE} + C_{LN} & -C_{LN} \\ -C_{LN} & C_{NE} + C_{LN} \end{bmatrix} \quad (16)$$

$$G = \begin{bmatrix} G_{LE} + G_{LN} & -G_{LN} \\ -G_{LN} & G_{NE} + G_{LN} \end{bmatrix} \quad (17)$$

For the distributed parameters obtained from (14) to (17), the impedance and propagation constant are

$$Z = \sqrt{(R_{MIMO} + j\omega L_{MIMO}) / (G_{MIMO} + j\omega C_{MIMO})} \quad (18)$$

$$\gamma = \sqrt{(R_{MIMO} + j\omega C_{MIMO})(G_{MIMO} + j\omega C_{MIMO})} \quad (19)$$

Here, ω is the angular frequency of the signal.

MIMO PLC CHANNEL MODELING

To design an effective PLC system, it is important to have an accurate Channel model. The top-down method is based on multipath propagation and can be modeled only with a large number of measurements. The problem of dynamic variation of loads cannot be addressed with this method.

The bottom-up approach of channel model can deal with any number of branches and with wide variety of loads. In this paper, a physical- deterministic model based on bottom-up approach is developed to estimate the CFR. The advantage of this method is the ease to handle the MIMO communication irrespective of the size and the complexity of the network.

The transmission line model of residential network can be represented as in Figure 3. It reflects the various domestic appliances connected to the multiple branches of the network. These appliances can be a light source, TV, refrigerator, ACs etc. Based on the load connected or the ampere rating of the plug socket, the cross-section of the wiring also differs. The wiring cross-section can be 1.5 mm² or 2.5mm² depending upon the load requirement. Another interesting aspect of the residential network is that these appliances are not continuously operated and this leads to variation in load impedance and attenuation of the network.

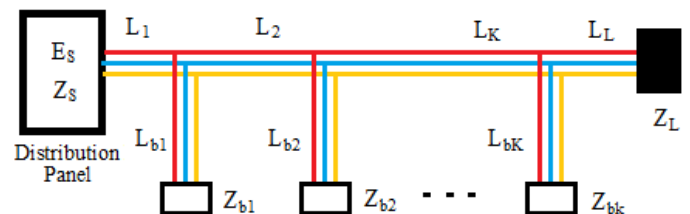


Figure 3: Transmission line model of indoor circuit

Here, Z_s is the internal impedance of the voltage source E_s . L_K ($K=1,..,n$) is the wire length between the branches. The internal impedance and propagation constant for the branches, with length L_{bK} ($K=1,..,n$) and load impedance Z_{bK} ($K=1,..,n$), are obtained using (18) and (19) respectively. For this,

The complex residential network can be simplified by applying the chain matrix theory. Using this, the complex multi-branch network can be divided into several parts and each part represented with a matrix. The first part will be the source and the last part will be load and the remaining parts will be separated at the branches. In other words, the second part will be from the source to the first branch, with the first branch included and the second branch will be between first branch and second branch, with the second branch included. These parts are obtained in matrix form using equation (9) to (12).

$$T_1 = \begin{bmatrix} 1 & Z_S \\ 0 & 1 \end{bmatrix} \quad (20)$$

$$T_2 = \begin{bmatrix} \cosh(\gamma_1 l_1) + \frac{Z_{01}}{Z_{ib1}} & Z_{01} \sinh(\gamma_1 l_1) \\ \frac{1}{Z_{01} \sinh(\gamma_1 l_1)} + \frac{\cosh(\gamma_1 l_1)}{Z_{ib1}} & \cosh(\gamma_1 l_1) \end{bmatrix} \quad (21)$$

$$T_{N+1} = \begin{bmatrix} \cosh(\gamma_N l_N) + \frac{Z_{0N}}{Z_{ibN}} & Z_{0N} \sinh(\gamma_N l_N) \\ \frac{1}{Z_{0N} \sinh(\gamma_N l_N)} + \frac{\cosh(\gamma_N l_N)}{Z_{ibN}} & \cosh(\gamma_N l_N) \end{bmatrix} \quad (22)$$

$$T_{N+2} = \begin{bmatrix} \cosh(\gamma_L l_L) + \frac{Z_{0L}}{Z_L} & Z_{0L} \sinh(\gamma_L l_L) \\ \frac{1}{Z_L \sinh(\gamma_L l_L)} + \frac{\cosh(\gamma_L l_L)}{Z_L} & \cosh(\gamma_L l_L) \end{bmatrix} \quad (23)$$

From the matrices obtained for each part, the whole network can be explained as

$$T = \prod_{i=1}^{N+2} T_i = \begin{bmatrix} T_{aa} & T_{ab} \\ T_{ba} & T_{bb} \end{bmatrix} \quad (24)$$

From the matrix obtained in (20) and using the transmission line theory, the CTF can be obtained by [6].

$$H(f) = Z_L / (T_{aa} Z_L + T_{ab} + T_{ba} Z_S Z_L + T_{bb} Z_S) \quad (25)$$

EXPERIMENTAL RESULTS

For characterizing the power line, the measuring devices are connected through a coupling interface to avoid any direct contact of the high voltage supply. The coupling circuit is also combined with surge protection devices (SPDs) to avoid unpredictable transients and surges.

A. Channel Frequency Response

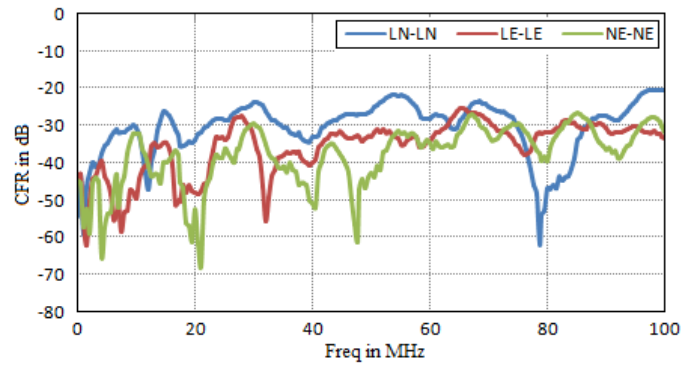


Figure 4: CFR for co-channels

In this section, the CFR of the power line is measured on all the three ports. The signal strength is measured on both co-channels and cross-channels. Co-channels are the one on which the data can be transmitted and received through the same ports and cross-channels are those on which the data is transmitted from a port and received from another ports. The measurements were carried out using a vector network analyser in the frequency range of 1-100 MHz and a carrier frequency of 500 kHz.

From the Fig. 4, it can be noticed that the CFR of LN-LN port is better than other ports. The NE-NE port can be of the least priority when a 2x2 MIMO communication has to be used.

Due to the coupling effect the data transmitted from a port will be received by the remaining ports and thus establishing a cross-channel communication. In the Fig. 5, it can be noticed that, for the signal transmitted from LN port, the CFR is better for LE receiver port than NE port. The observations from Fig. 4 and Fig. 5 are confirmed from the literature [7].

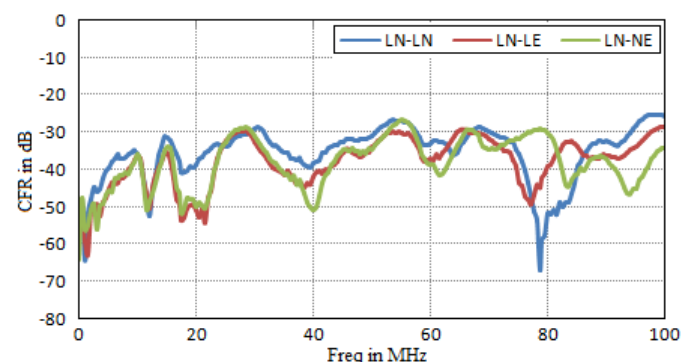


Figure 5: CFR for cross-channels

B. Stationary noise

This stationary noise or background noise is a result of noise produced by the electrical appliances. These disturbances vary with time and will affect the maximum achievable transmission rate of the channel. The noise in the power line is

measured in the frequency range of 1-100 MHz using a spectrum analyzer. A total of 200 noise measurements on LN, LE and NE are recorded for every 15 minutes.

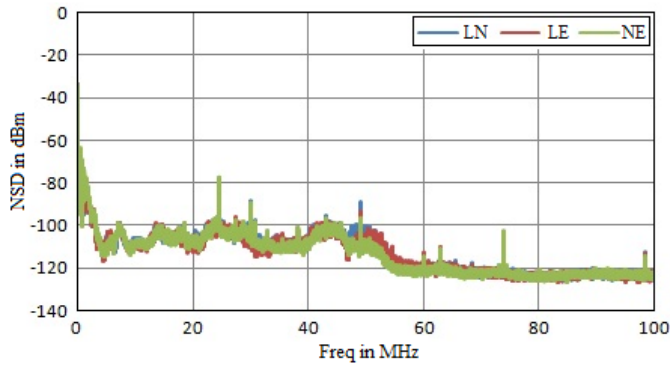


Figure 6: Stationary noise on all the three ports

The noise spectrum density (NSD) is captured with 8192 sweep points on all the three ports and is as shown in Fig. 6. The stationary noise can be modeled using the Esmailian model and is represented as [13].

$$S(f) = a + bf^c \quad (26)$$

Here, the parameters, a, b, c represent the variation in noise due to time and location. The statistical parameters of these values are for L, LE and NE are shown in Table I.

TABLE I. STATISTICAL PARAMETERS OF STATIONARY NOISE

	a	b	c
Stationary Noise in L-N			
Min	306946	-0.72	126.18
Max	2197168	-0.6	128.5
Average	957865	-0.66	127.0
Standard Deviation	487653	0.03	0.505
Stationary Noise in L-E			
Min	187898	-0.74	126.0
Max	2688913	-0.56	127.8
Average	1134584	-0.66	126.9
Standard Deviation	649892	0.042	0.4
Stationary Noise in N-E			
Min	399336	-0.74	126.3
Max	2785355	-0.61	127.8
Average	1355489	-0.68	126.8
Standard Deviation	703397	0.036	0.33

From the figure, it can be noticed that, the LE channel is less affected when compared to other channels. The radio interference can also be noticed on all the channels.

C. Impulsive noise

The appliances connected to the network will exhibit impulsive noises on the channel. These disturbances are very dynamic in nature and are in the form of single pulse or repetitive pulse with short durations and are either damped sinusoids or exponential sinusoids.

The experiment was carried out on 15 different sockets of all the three ports of the residence using a Digital oscilloscope at a sampling frequency of 1.25 Gs/sec. The statistical parameters of the impulsive noise is as shown in Table II.

TABLE II. STATISTICAL PARAMETERS OF IMPULSIVE NOISE

	Pulse Width (ms)	Duration (ms)	Amplitude (mV)
Impulsive Noise in L-N			
Min	0.82	1.2	17.2
Max	3.48	19.65	52
Average	1.677	5.75	34.58
Standard Deviation	0.627	3.807	9.87
Impulsive Noise in L-E			
Min	0.74	0.98	17.8
Max	1.78	4.92	31.2
Average	1.45	2.10	26.2
Standard Deviation	0.48	1.88	5.94
Impulsive Noise in N-E			
Min	1.3	1.46	14.2
Max	4.38	9.6	54
Average	2.42	5.04	36.18
Standard Deviation	0.80	2.66	12.075

SIMULATION AND RESULTS

A. Channel Frequency Response

For simulating the CFR, a fire retardant stranded house wire of 2.5 sq.mm and an insulation thickness of 0.8 mm is assumed

across the network. The conduit size is of ½” with the branches scattered throughout the length.

For the 2x2 PLC channel model, the CFR of LN-LN and LN-LE port are simulated and is shown in Fig. 7. The results obtained from simulation and the experimental results as per Fig. 5 confirm that port LN-LN has the least signal attenuation.

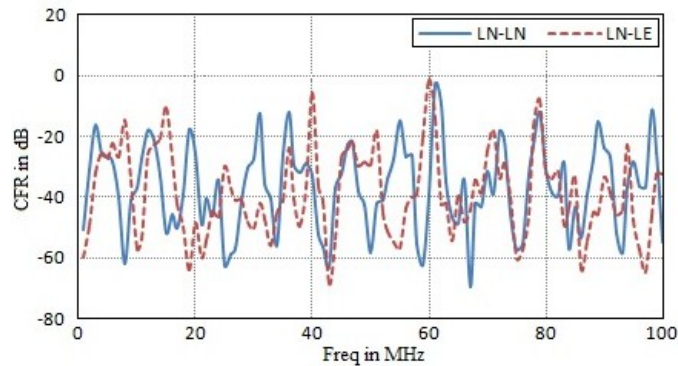


Figure 7: Simulated CFR of MIMO PLC

The phase response of the simulated channel generator is also shown in Fig. 8.

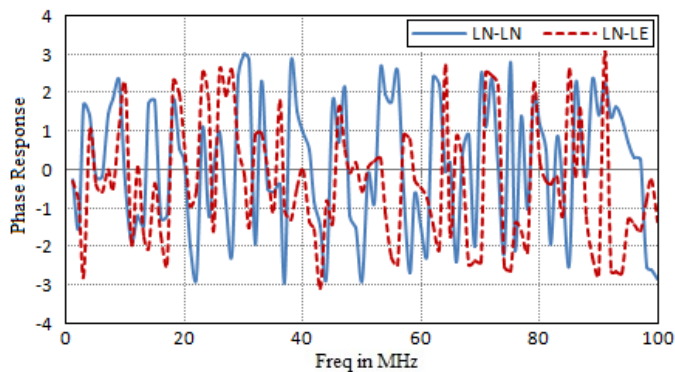


Figure 8: Simulated phase response of MIMO PLC

B. Channel Capacity

The maximum possible transmission rate of a PLC channel can be realized by estimating the channel capacity. The Channel capacity for a SISO channel is given as [14].

$$C_{SISO} = \Delta f \cdot \sum_{n=1}^L \log_2 \left[1 + \frac{P(f_n) |H(f_n)|^2}{N(f_n)} \right] \text{ bit/s} \quad (27)$$

Here P(f) and N(f) are PSD and NSD in dBm/Hz at transmitter and receiver ports respectively. Δf and L are the carrier width and number of carriers.

These values are obtained from the experimental results and the statistical modeling carried out and is shown in Table III.

TABLE III. CHANNEL PARAMETERS

	Values
Frequency band	1-100 MHz
Carrier width (Δf)	500 kHz
Number of carriers (L)	200
PSD (P(f))	-93 dBm/Hz
NSD (N(f))	-128.4 for L-N
	-127.7 for L-E

For a 2x2 MIMO Channel, the estimation of Channel capacity is explained in [14]:

$$C_{MIMO} = \Delta f \cdot \left\{ \log_2 \left[\det \left(I_{n_R} + \frac{SNR}{n_T} H H^H \right) \right] \right\} \quad (28)$$

For a MIMO PLC system with LN, LE has transmitter and receiver ports, the channel matrix can be written as

$$H = \begin{bmatrix} H_{LN-LN} & H_{LN-LE} \\ H_{LE-LN} & H_{LE-LE} \end{bmatrix} \quad (29)$$

The channel capacity for MIMO PLC can be obtained by diagonalizing the product matrix of HH^H using singular value decomposition (SVD).

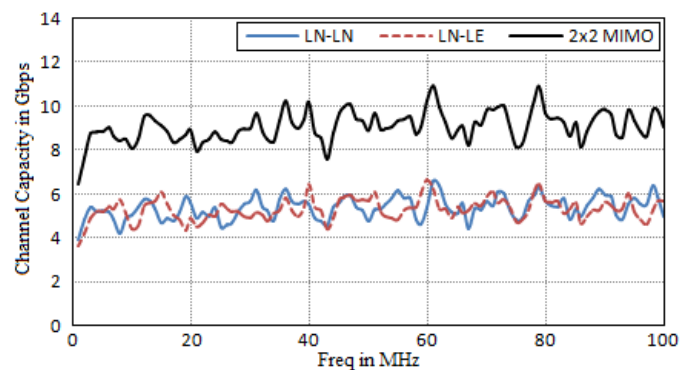


Figure 9: Comparison of channel capacity

A considerable increase in channel capacity is noticed when a MIMO PLC is used. The minimum capacity of 2x2 MIMO

channel is 6.45 Gbps and for LN-LN and LN-LE port is 3.95 Gbps and 3.6 Gbps respectively. The maximum capacity of 2x2 MIMO channel is 10 Gbps and for both LN-LN and LN-LE port is 6.6 Gbps. The average channel capacity of 2x2 MIMO channel is 9 Gbps and for both LN-LN and LN-LE port is 5.3 Gbps.

C. Average Channel Gain

The ACG can be expressed as the average attenuation and is expressed as

$$ACG_{dB} = 10 \log_{10} \left(B \frac{1}{f_2 - f_1} \int_{f_1}^{f_2} |H(f)| df \right) \quad (30)$$

For the CFR $H(f)$, f_1 and f_2 are at 0.5 MHz and 100 MHz respectively. For the simulated CFRs, the average channel gain of LN-LN is 31.93 dB and for LN-LE is 32.35 dB.

CONCLUSION

A detailed analysis is carried out on the Indian residential networks for characterizing the MIMO power line channel. Though the channel transfer function is developed based on the multi-conductor transmission line theory, the noise in the channel is modeled on statistical analysis. From the results, a significant increase in the channel capacity is noticed for a 2x2 MIMO system as compared to the SISO communication channels. The Average Channel Gain is also proved to be same for both experimental and simulated CFRs. This value is equal to the ACG estimated for Brazilian In-home PLC channels [15].

REFERENCES

[1] Lars T.Berger, Andreas Schwager and Daniel M.Schneider, "MIMO Power line Communications," IEEE communication survey & Tutorials Vol 17, No.1, pp. 106-123, 2015.

[2] European Telecommunication Standards Institute (ETSI), "Powerline Telecommunications (PLT); MIMO PLT; Part 1: Measurement methods of MIMO PLT," Sophia-Antipolis Cedex, France, ETSI TR 101 562-1, Feb. 2012.

[3] European Telecommunication Standards Institute (ETSI), "Powerline Telecommunications (PLT); MIMO PLT; Part 2: Setup and statistical results of MIMO PLT EMI measurements," Sophia-Antipolis Cedex, France, ETSI TR 101 562-2, Oct. 2012

[4] European Telecommunication Standards Institute (ETSI), "Powerline Telecommunications (PLT); MIMO PLT; Part 3: Setup and statistical results of MIMO PLT channel and noise measurements," Sophia-Antipolis

Cedex, France, ETSI TR 101 562-3, Feb. 2012.

[5] Shashidhar Kasthala and GKD Prasanna Venkatesan, "Evaluation of Channel modeling techniques for Indoor Power Line Communication," International Conference on Advanced Computing and Intelligent Engineering, Bhubaneswar, India, December 2016.

[6] J.A.Cortes', L.Diéz, F.J.Cañete and J.L.G.Moreno, "On the statistical properties of indoor power line channels: Measurements and models," IEEE International symposium on Power-Line Communications and its Applications, April 2011, pp.271-276.

[7] Julio A.Corchado, "An MTL based channel model for Indoor Broadband MIMO Power Line communications," IEEE journal of selected areas of communication, Vol. 34, No. 7, pp. 2045-2055, Jul 2016.

[8] F. Rousissi, H. Gassara, A.Ghazel and S.Najjar, "Comparative study of impulsive noise models in the narrowband Indoor PLC environment," Tenth workshop on the power line communication, 10-11 October 2016.

[9] Shashidhar Kasthala and GKD Prasanna Venkatesan, "Experimental verification of distributed parameters on indian residential networks for power line communication," International Journal of Engineering & Technology, vol 8, Issue. 6 2016.

[10] R.Hashmat, P.Pagani, and T.Chonavel, "MIMO communications for inhome PLC networks: Measurements and results upto 100 MHz," in Proc. IEEE Int. Symp. Power Line Commun. Appl., Rio de janeiro, Brazil, Mar. 2010, pp 120-124.

[11] Clayton R.Paul, Analysis of Multiconductor Transmission Lines, John Wiley & Sons, Inc, pp.46-62, 2004.

[12] Despina Anastasiadou, Theodore Antonakopoulos, "An Experimental Setup for Characterizing the Residential Power Grid variable behavior", Proceedings of the 6th International Symposium on Power Line Communications and its Applications, Athenes, Greece, March 27-29, 2002.

[13] T.Esmailian, P.G.Gulak and F.R.Kschischang, "A discrete multitone power line communication system," Proceedings of ICASSP'00, Vol. 5, pp. 2953-2956, Jun 2000.

[14] Bengt Holter, "On the capacity of MIMO Channel-A tutorial Introduction", Norwegian University of Science & Technology.

[15] Thiago R.Oliveira, Camila B.Zellar Sergio L.Netto and Moises V.Ribeiro, "Statistical Modeling of the Average Channel Gain and Delay Spread in In-Home PLC Channels," IEEE International symposium on Power Line Communication and its Applications, 2015.